

The Analysis of Surrounding Structure Effect on the Core Degradation Progress with COMPASS Code

Jun Ho Bae*, Dong Gun Son, Jong Tae Kim, Rae Jun Park, Dong Ha Kim

Korea Atomic Energy Research Institute P.O.Box 105, Yusong, Daejeon, 305-600, Korea

*Corresponding author: bjh@kaeri.re.kr

1. Introduction

In line with the importance of severe accident analysis after Fukushima accident, the development of integrated severe accident code has been launched by the collaboration of three institutes in Korea. KAERI is responsible to develop modules related to the in-vessel phenomena, while other institutes are to the containment and severe accident mitigation facility, respectively. In the first phase, the individual severe accident module has been developed and the construction of integrated analysis code is planned to perform in the second phase. The basic strategy is to extend the design basis analysis codes of SPACE and CAP, which are being validated in Korea for the severe accident analysis [1]. In the first phase, KAERI has targeted to develop the framework of severe accident code, COMPASS (COre Meltdown Progression Accident Simulation Software), covering the severe accident progression in a vessel from a core heat-up to a vessel failure as a stand-alone fashion.

2. Computational Procedure

The core is represented by multiple parallel channels and each channel has a prescribed number of fuel elements and the associated coolant channel. The thermal-hydraulic model has been developed for the each component of coolant, cladding and fuel rod in a node. The mixture model for coolant temperature has been used and the relationship between a void fraction and a quality has been derived from the force balance between the drag and buoyancy forces. The inlet flow rates of multiple channels are determined by the equivalence of pressure drop between the neighboring channels. The flow rate and enthalpy of coolant are calculated from the mass and energy conservation equations for each node. As a core heats up by the decrease of flow rate, the clad temperature reaches the oxidation temperature and Zircaloy becomes to change as Zirconium dioxide (ZrO_2) by the oxidation with the high temperature vapor, which means the decrease of metallic Zircaloy mass with the increase of ZrO_2 mass. At the same time, the heat generation due to the oxidation reaction increases the clad temperature steeply. When the cladding temperature reaches the melting temperature of Zircaloy, it starts to melt and relocates to the lower node. The continued temperature increase results to the melting of ZrO_2 and uranium, sequentially. The melted ZrO_2 and uranium relocates to

the lower node and they are frozen at the lower node before the node reaches the melting temperature of each material. The continued mass relocation generates a molten pool at a certain node after the frozen mass blocks the coolant flow area. After then, the melted mass is stacked on the molten pool until the blocked frozen mass starts to melt. Besides the relocation due to the material melting, the slumping of solid material is also considered in the relocation model. The slumping is assumed to occur before the clad temperature reaches to the melting temperature of Zircaloy due to the weakness of solid structure. Since the relocated mass due to the melting and slumping affects to the energy of the lower node, it is reflected to the energy conservation equation of each node. The molten pool is finally formed above the lower core support plate and the molten corium of core becomes to relocate to the lower plenum when the lower core support plate fails due to the increased temperature and weight [2].

3. Calculation Results

In order to analyze the effect of surrounding structure, the melt progression has been compared between the central zone and the most outer zone under the condition of constant radial power peaking factor. Figure 2 and 3 shows the fuel element temperature and the clad mass at the central zone, respectively. Due to the axial power peaking factor, the axial node #3 has the highest temperature, while the top and bottom nodes have the lowest temperature. When the clad temperature reaches to the Zr melting temperature (2129.15K), the Zr starts to melt. The axial node #3 starts to melt about 3500sec and the molten Zr mass relocates to the axial node #2 (In Fig.3, the clad mass of node #3 decrease with the increase of clad mass of node #2). And, the clad temperature at the axial node #2 reaches to ZrO_2 melting temperature (2973.15K) about 4400sec and starts to melt.

Similarly, the axial node #2 starts to melt about 3900sec and the molten Zr mass relocates to the axial node #1 which results to the increase of clad mass and temperature of node #1. Axial node #1 reaches to the Zr melting temperature about 5000sec and the clad mass starts to decrease by the melting of Zr mass. And it reaches to the ZrO_2 melting temperature about 5300sec, which results to the clad mass decreases to zero about 5600sec. Figure 3 shows the flow area variation by the molten mass relocation. It is shown that the axial node #1 is blocked about 5200sec, which has the zero flow

area. The axial node #2 reaches to the fuel melting temperature about 5000sec and the molten fuel relocates to the node #1, which results to the blockage of flow area in node #1. The blocked flow area becomes to open about 6100sec due to the molten ZrO₂ mass relocation to core support plate.

Figure 4 and 5 shows the fuel element temperature and the clad mass at the most outer zone, respectively. It is shown that the fuel temperature increase more slowly compared with the central zone since the most outer zone has the heat loss to surrounding structure. Figure 6 shows the flow area at the most outer zone. Since the axial node #1 reaches to the ZrO₂ melting temperature soon after the above nodes reaches to the ZrO₂ melting temperature, which results the node #1 not to be blocked due to the ZrO₂ melting of node #1.

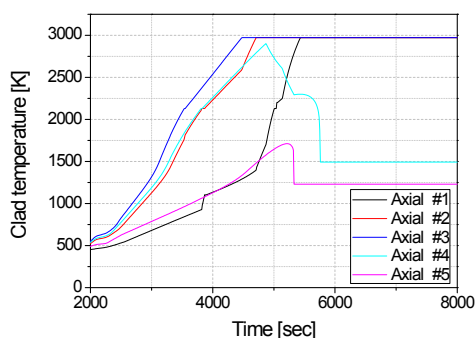


Fig.1 The clad temperature at the central zone

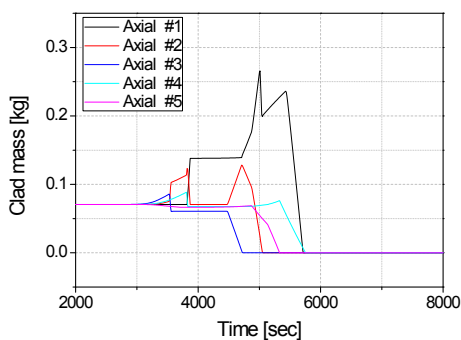


Fig.2 The clad mass at the central zone

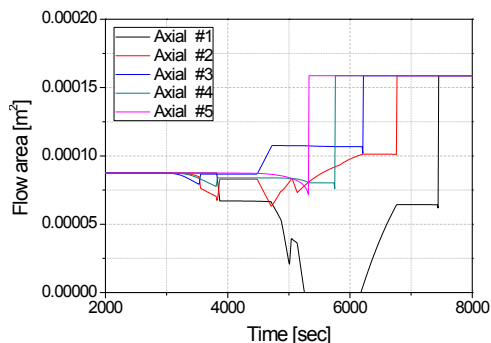


Fig.3 The flow area variation at the central zone

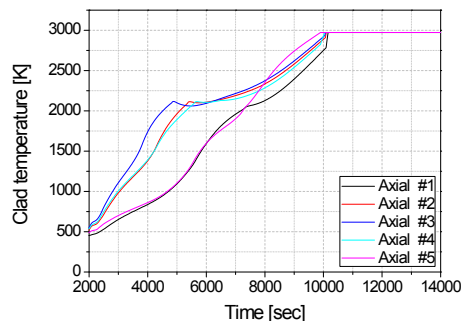


Fig.4 The clad temperature at the most outer zone

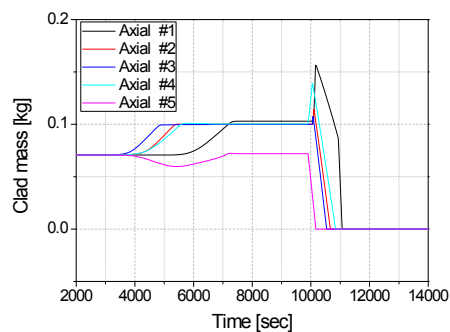


Fig.5 The clad mass at the most outer zone

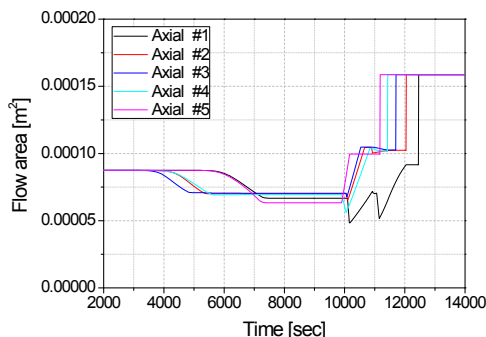


Fig.6 The flow area variation at the most outer zone.

ACKNOWLEDGMENT

This work was supported by the Nuclear & Development of the Korea Institute of Energy Technology Evaluation and Planning (KETEP) grant funded by the Korean government (Ministry of Trade, Industry, and Energy) (No. 20141510101671)

REFERENCES

- [1] S.J. Ha, C.E. Park, K.D. Kim, C.H. Ban, "Development of the SPACE code for Nuclear Power Plant", Nuclear Engineering and Technology, Vol.43. pp. 45-62 (2011)
- [2] J.H. Bae, J.H. Park, R.J. Park, D.H. Kim, "The Programmer Manual for the Core Degradation Module", KAERI/TR-5700/2014 (2014)